

Experimental Characterization of Chua's Circuit

Majid Sodagar,¹ Patrick Chang,¹ Edward Coyler,¹ and John Parke¹

School of Physics, Georgia Institute of Technology, Atlanta, Georgia 30332, USA

(Dated: 13 December 2012)

In this work we have hooked up the Chua's circuit and attempted to characterize the behaviour of the system by reconstructing the attractor and calculating the correlation dimension from the experimental data. Also we estimated the Lyapunov exponent of the system and tried to extract an iterative map. Finally we compared our measurement and calculations with simulation results.

I. INTRODUCTION

Chua's circuit is an autonomous electronic circuit capable of having chaotic behaviour which was first introduced at 1983. The original circuit contains a resonant tank part including a capacitor and inductor and a nonlinear part containing a piecewise linear diode. It has been shown that the nonlinear part can assume different forms^{1 2 3}. In figure 1 a generic schematic of such a circuit is provided. This circuit has three energy

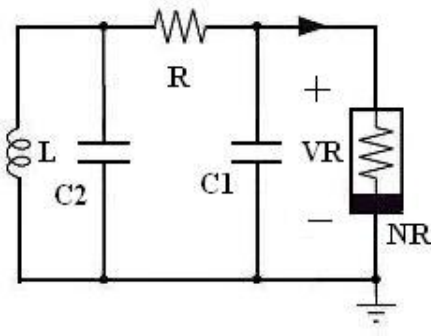


FIG. 1. Generic schematic of Chua's circuit

saving elements (two capacitors and one inductor) and hence the governing differential equation is of third order. It has been shown that by replacing the resonant tank with a higher order RCL ladder one can get a higher order chaotic nonlinear differential equation⁴, so this circuit can also be useful for investigating higher order chaotic systems.

There are several applications that one might envision for such a system among which are secure telecommunication^{5 6}, trajectory recognition⁷, handwritten character recognition⁸ and music synthesizer⁹. In this work we have chosen a piecewise linear active resistor realized by two operational amplifiers as the nonlinear part of the circuit. The schematic diagram of the nonlinear part is shown in figure 2a. Here we used two op-amps to mimic a piecewise active resistor. The general characteristics of such a circuit is shown in figure 2b.

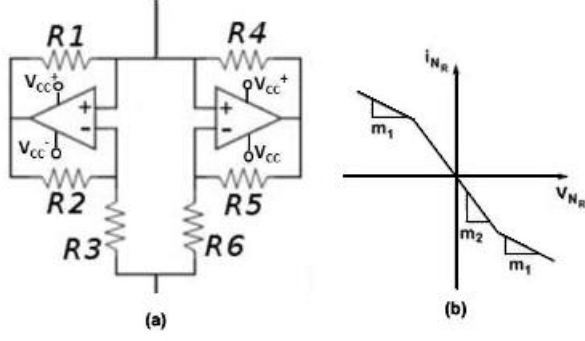


FIG. 2. Piecewise linear active resistor circuit

The actual values for elements in this circuit which are used in this work is as follows: $R=10k$ potentiometer, $R1=220$, $R2=220$, $R3=2.2k$, $R4=22.0k$, $R5=22.0k$, $R6=3.3k$, $L=15mH$, $C1=10nF$, $C2=100nF$.

The associated governing equations for voltages and currents can readily be written using Kirchoff's laws which after transforming into dimensionless form as follows¹⁰:

$$\frac{dx}{d\tau} = \alpha(y - x - f(x)), \quad \frac{dy}{d\tau} = y - x, \quad \frac{dz}{d\tau} = -\beta y. \quad (1)$$

where

$$f(x) = \begin{cases} m_1 x + m_0 - m_1, & x > 1 \\ m_0 x, & -1 \leq x \leq 1, \\ m_1 x - m_0 + m_1, & x < -1 \end{cases} \quad (2)$$

and

$$x \equiv \frac{V_{c1}}{B_p}, \tau \equiv \frac{tG}{C_2}, \alpha \equiv \frac{C_1}{C_2}, y \equiv \frac{V_{c2}}{B_p},$$

$$m_0 \equiv \frac{G_a}{G}, \beta \equiv \frac{C_2}{LG^2}, z \equiv \frac{i_L}{B_p G}, m_1 \equiv \frac{G_b}{G}.$$

It is obvious that by changing the value of our potentiometer we can change m_0 and

m_1 . Also it has been shown¹⁰ that in order to have a period doubling route to chaos we should have $m_0 < -1$ and $-1 < m_1 < 0$.

To measure the actual values for G_a and G_b we added a 868k resistor in series with this circuit and hooked it up with a sinusoidal wave generator and measured the voltage drop across the nonlinear active resistor. Figure 3 depicts the voltage drop across the piecewise linear resistor versus the voltage source. Using this graph we could calculate the G_a and G_b values to be $-7.5372e-004 \Omega^{-1}$ and $-6.6965e-004 \Omega^{-1}$ respectively.

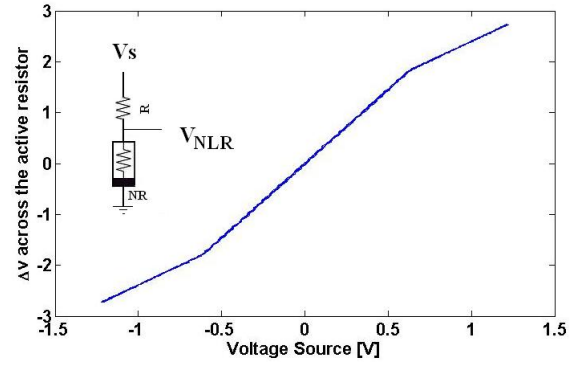


FIG. 3. Piecewise linear active resistor circuit

Given these values we can calculate m_0 and m_1 for different values of G . Figure 4 show that in our setup the route to chaos is definitely not period doubling for any value of the potentiometer. Instead, we observed periodic behaviour, screw attractor, followed by a double scroll as the resistance of the potentiometer was increased. In the rest of our experiment we measured two phase space variables out of three, i.e. voltages across the

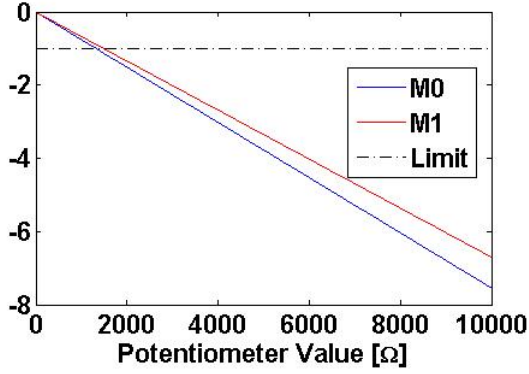


FIG. 4. Calculated m_0 and m_1 versus potentiometer resistance

two capacitors. In the following section we will discuss methods of attractor reconstruction and fractal dimension estimation along with the Lyapunov exponent. Afterwards we will compare our results with simulation.

II. METHODS

We have used the time delayed method to reconstruct the attractor in the phase space. In this method reconstruction is based on the measurement of only one phase variable. Then the topological replica of the attractor can be reproduced by considering $X(t), X(t+\tau), X(t+2\tau), \dots, X(t+2n\tau)$ wherein n is the embedding dimension of the phase space. There are several methods to estimate τ among which is a powerful method based on an information theoretic concept¹¹. In this method the mutual information between $X(t)$ and $X(t+\tau)$ needs to be calculated as a func-

tion of τ as follows:

$$I(\tau) = - \sum_{h,k=1}^j P_{h,k}(\tau) \ln \frac{P_{h,k}(\tau)}{P_h P_k} \quad (3)$$

Assuming that the range of the signal is divided into N sections and X_i s are the samples of the signal, P_h and P_k would denote the probabilities that X_i assumes a value inside the h th and k th sections respectively. Also $P_{h,k}(\tau)$ is the joint probability that X_i and $X_{i+\tau}$ are in sections h and k .

The optimum value for τ then would be the smallest possible values which minimizes $I(\tau)$. Here we will choose $X(t)$ to be the voltage across one of the capacitors (V_{c1}). Figure 5 shows the time domain sampled version of the voltage signals where the sampling rate was set to 24KHz. Also we will use the correla-

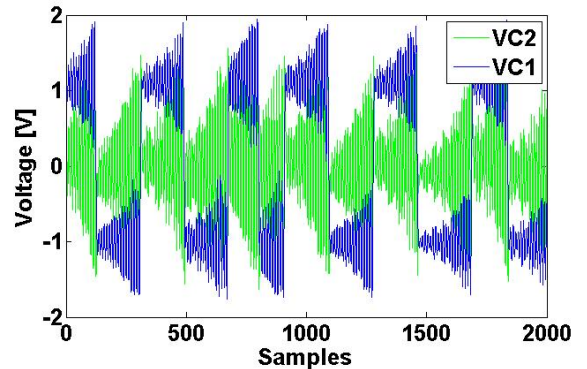


FIG. 5. Time domain voltage signals sampled at 24KHz

tion dimension concept to estimate the fractal dimension of the attractor. Having a finite number of points (N) on the attractor one can find the correlation dimension by evaluation

the following mathematical formation:

$$C(R) = \lim_{N \rightarrow \infty} \frac{1}{N^2} \sum_{i,j=1}^N H(R - |X_i - X_j|) \quad (4)$$

The slope of capacity (C) versus radius (R) in log scale will be the correlation dimension.

Regarding the Lyapunov exponents we used two trajectories with close initial conditions for each attractor (double scroll and screw attractor). We used our experimental data to estimate the Lyapunov exponents by evaluation the following formula¹²:

$$\lambda = \frac{1}{\Delta t} \ln \frac{\delta X(t = \Delta t)}{\delta X_0(t = 0)} \quad (5)$$

Here δX_0 is the difference between initial conditions and $\delta X(t)$ is the divergence of the trajectory after Δt is passed. Regarding the fact that Δt is finite, this definition implies that the might depend on the initial condition as well. We took an average over several initial conditions to get a more realistic estimation. Figure 6 depicts the measured

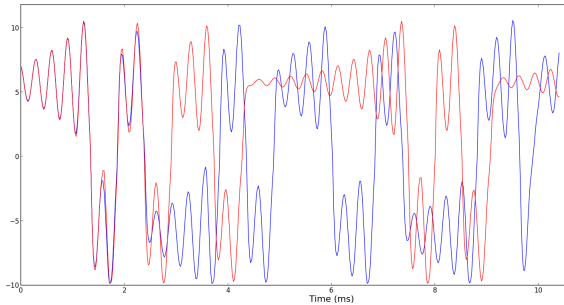


FIG. 6. Trajectories with close initial conditions data of two trajectories with a rather close initial conditions. Nearby trajectories were

obtained by tracing though the data and finding two points in phase space that were closer than 0.0075 Volt.

III. RESULTS

We used equation (3) to estimate the mutual information. In this calculation the signal range was divided in 100 sections. Figure 7 shows the mutual information calculated for the signal shown in figure(5). Its obvious that the first minimum occurs for τ equal to 3.

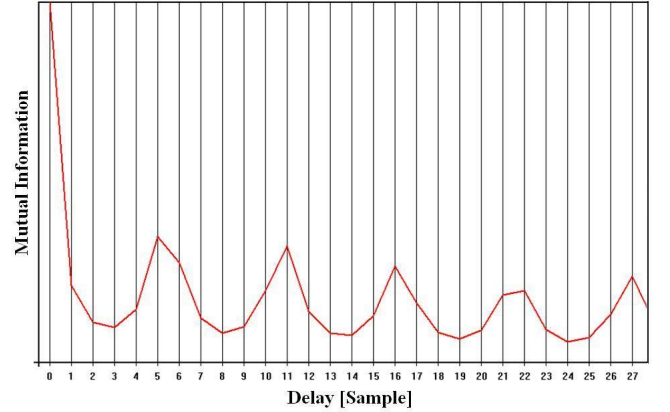


FIG. 7. Mutual Information vs. delay

Having the optimum delay we can now reconstruct the topological equivalent of the attractor in 2D and 3D. Figure 8 shows the 2D reconstructed attractor using the time delay method along with the measured attractor obtained by measuring the voltages across two capacitors. In comparison with the measured 2D attractor we see that most features in the real attractor are preserved and that

the only major difference is a rotation in the plane which will not change the fractal dimension of the attractor and does not have any significance.

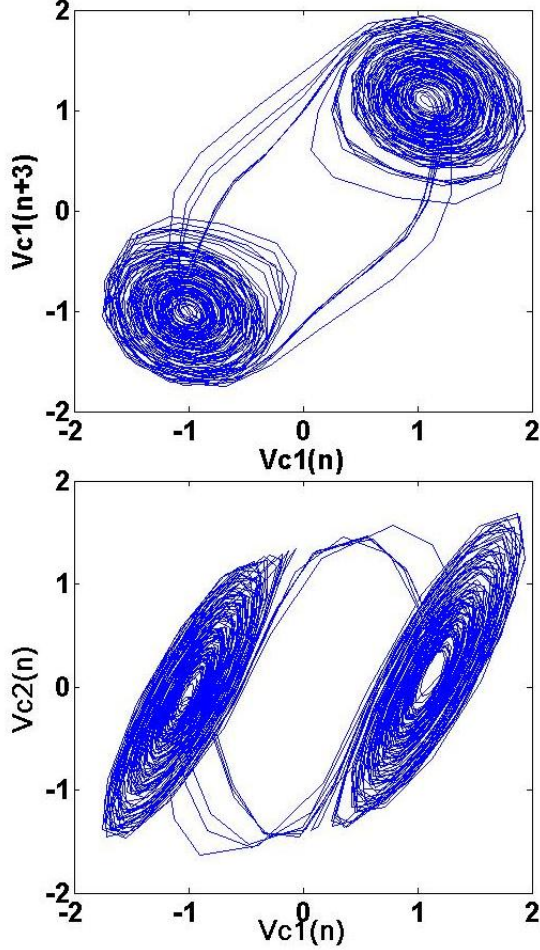


FIG. 8. Reconstructed (up) and Measured (Down) attractor

Figure 9 is the angled view of the reconstructed attractor in 3D.

Figure 10 shows the capacity versus radius in log scale calculated using equation (4) for the reconstructed attractor shown in figure (7). There are two saturation regions for large and small values of R which are due to

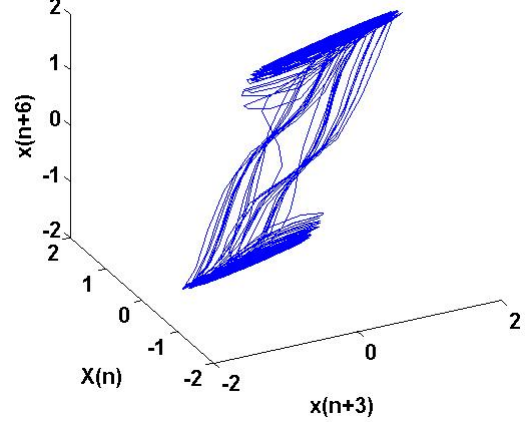


FIG. 9. Reconstructed Attractor in 3D

the fact that the attractor is contained in a finite region in space and also the trajectory resolution is limited by the sampling rate. Form this graph the correlation dimension is estimated to be 1.85. Note that for this estimation we have used 4000 data points on the trajectory. By increasing the data points this slope slightly increases and approaches to 1.9 which is in good agreement with other works¹³.

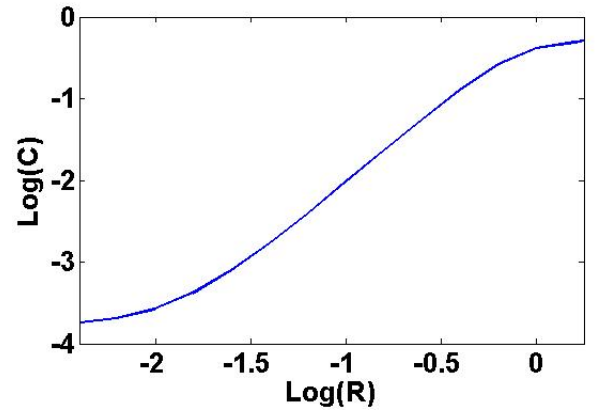


FIG. 10. Correlation dimension

In figure 11 show the Lyapunov exponent

for the double scroll attractor for a random initial condition. As you see there are lots of fluctuations on this curve. Still Lyapunov exponent can be estimated by measuring the slope of a line fitting the curve. For this specific initial condition the slope was measured to be 1.15. This procedure was done for a number of initial conditions. we got the arithmetic average of 1.33 with a standard deviation of 0.3.

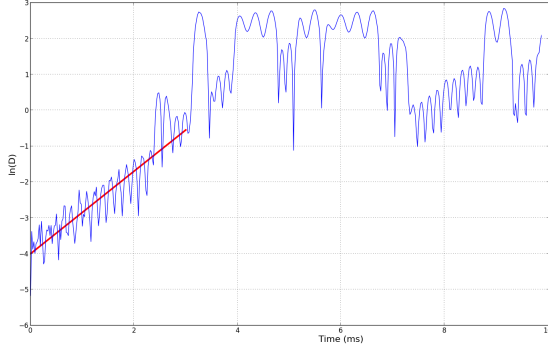


FIG. 11. Lyapunov exponent estimation

Note that there the saturation in this graph is again due to the fact that the trajectories are confined to the double scroll. We also attempted to extract an iterative map by using the local maxima of the the signal corresponding to different conditions of the circuit. The extracted maps look strange and we can not explain its general behaviour. Figure 12 shows one of such maps.

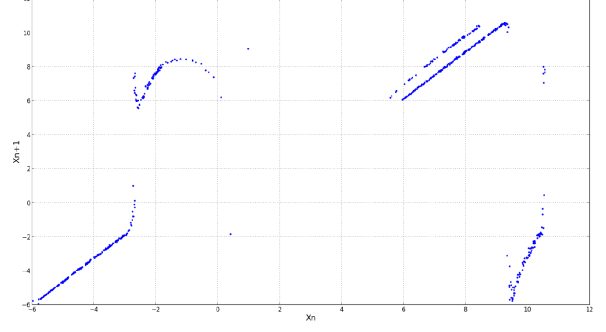


FIG. 12. Iterative map extracted from V_{c1}

IV. SIMULATION

In this section we used direct numerical integration of the differential equations in (1) and compare the results with what we have measured. Figure 13 shows the three phase space variables, i.e. the two capacitor voltages and the inductor current. the general behaviour of the two voltages is similar to that of our measurement in figure 5.

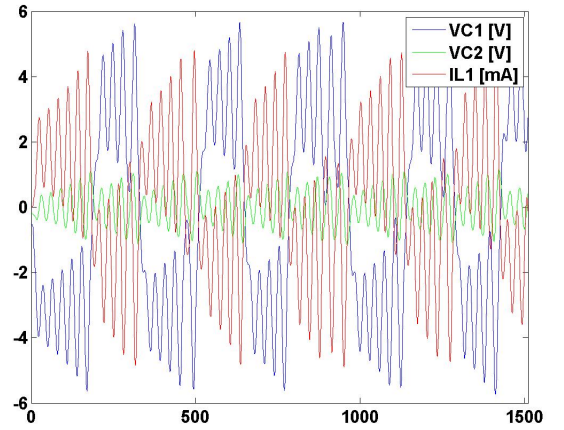


FIG. 13. Simulated phase space variable in time domain

Figure 14 depicts the 2D attractor in the

phase space which is also comparable to that of measured and reconstructed in figure 8. The same result holds for the 3D attractor.

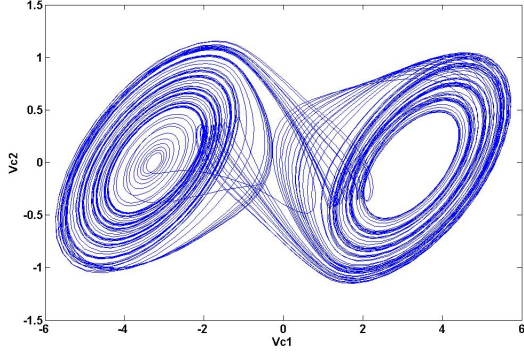


FIG. 14. Simulated 2D attractor

We also repeated the same algorithm to calculate the correlation dimension of the attractor using simulated data this time with lower data points. Result is shown in figure 15 with the slope of 1.84 which is in good agreement with what we got in figure 10.

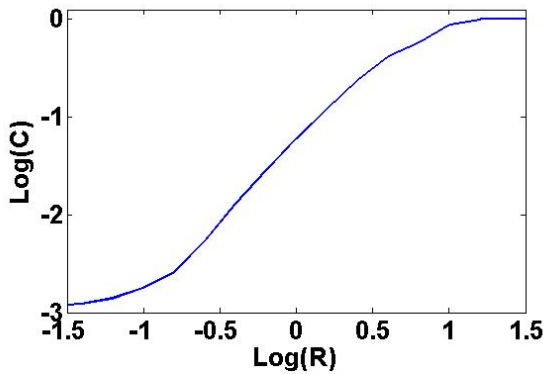


FIG. 15. correlation dimension extracted from Simulated Data

V. CONCLUSION

In this work we have successfully set up a nonlinear chaotic circuit and could measure two phase space variables out of two. To characterize the circuit we first attempted to reconstruct the attractor using time delay method benefiting from an information theoretic concept to estimate the time delay. Also we estimated the Lyapunov exponent of the system and fractal dimension of the attractor using correlation dimension which turned out to be in good agreement with the published data. Considering Kirchoff's laws we could model the circuit mathematically and solved the differential equations using numerical methods. Our experimental results are in good agreement with what simulation suggests. This project can be followed by further investigation of other mathematical measures of fractals and chaotic systems. Also one can try to synchronize two of such chaotic circuits and use them as the basic components for realization of a simple secure communication system. Higher order chaotic system can readily be implemented by a simple extension to the RC tank as well. Also by choosing the right set of parameters for electronic elements one can achieve period doubling route to chaos that can be put into test.

REFERENCES

- ¹I. Adelheid, G. Álvaro, and B. Palhares, “Chua’s circuit with a discontinuous non-linearity,” *Journal of Circuits, Systems, and Computers* **3**, 231–237 (1993).
- ²R. Brown, “From the chua circuit to the generalized chua map,” *Journal of Circuits, Systems, and Computers* **3**, 11–32 (1993).
- ³A. E. J., “Bifurcation analysis of chua’s circuit with application for low level visual sensing altman,” *Journal of Circuits, Systems, and Computers* **3**, 63–92 (1993).
- ⁴L. Kocarev, L. Karadzinov, and L. Chua, “n-dimensional canonical chua’s circuit,” *Journal of Circuits, Systems, and Computers* **3**, 239–258 (1993).
- ⁵H. Dedieu, M. Kennedy, and M. Hasler, “Chaos shift keying: modulation and demodulation of a chaotic carrier using self-synchronizing chua’s circuits,” *Circuits and systems II: Analog and digital signal processing*, *IEEE Transactions on* **40**, 634–642 (1993).
- ⁶W. CHAI and O. LEON, “A simple way to synchronize chaotic systems with applications to secure communication systems,” *International Journal of Bifurcation and Chaos* **3**, 1619–1627 (1993).
- ⁷E. Altman, “Normal form analysis of chua’s circuit with applications for trajectory recognition,” *Circuits and Systems II: Analog and Digital Signal Processing*, *IEEE Transactions on* **40**, 675–682 (1993).
- ⁸B. Baird, M. Hirsch, and F. Eeckman, “A neural network associative memory for handwritten character recognition using multiple chua characters,” *Circuits and Systems II: Analog and Digital Signal Processing*, *IEEE Transactions on* **40**, 667–674 (1993).
- ⁹X. Rodet, “Models of musical instruments from chua’s circuit with time delay,” *Circuits and Systems II: Analog and Digital Signal Processing*, *IEEE Transactions on* **40**, 696–701 (1993).
- ¹⁰L. Chua and L. Huynh, “Bifurcation analysis of chua’s circuit,” in *Circuits and Systems, 1992., Proceedings of the 35th Midwest Symposium on* (IEEE, 1992) pp. 746–751.
- ¹¹A. Fraser and H. Swinney, “Independent coordinates for strange attractors from mutual information,” *Physical review A* **33**, 1134 (1986).
- ¹²S. Strogatz, “Nonlinear dynamics and chaos: with applications to physics, biology, chemistry and engineering,” (2001).
- ¹³G. Lin, “A universal circuit for studying chaos in chua’s circuit family,” in *Circuits and Systems, 1991., Proceedings of the 34th Midwest Symposium on* (IEEE, 1991) pp. 772–775.